

# Fabrication of miniature Clark oxygen sensor integrated with microstructure

Ching-Chou Wu, Tomoyuki Yasukawa, Hitoshi Shiku, Tomokazu Matsue\*

*Graduate School of Environmental Studies, Tohoku University, Aramaki 07, Aoba, Sendai 980-8579, Japan*

Received 3 October 2004; received in revised form 18 January 2005; accepted 6 February 2005

Available online 3 March 2005

## Abstract

A miniature Clark-type oxygen sensor has been integrated with a microstructure using a novel fabrication technique. The oxygen chip consists of a glass substrate with a three-electrode configuration, which is separated and connected by a groove, and a poly(dimethylsiloxane) (PDMS) container with an immobilized PDMS oxygen-permeable membrane. The assembly of the different substrates only uses the O<sub>2</sub> plasma bonding technique, and the fabrication temperatures do not exceed 95 °C. Characteristics of the miniature sensor include the fastest response time of 6.8 s, good linearity with a correlation coefficient of 0.995, and a long lifetime of at least 60 h. The present miniature Clark oxygen sensor can be readily integrated with a microfluidic system to form a  $\mu$ -TAS.

© 2005 Elsevier B.V. All rights reserved.

**Keywords:** Clark oxygen sensor; Miniaturization; O<sub>2</sub> plasma bonding;  $\mu$ -TAS; Poly(dimethylsiloxane)

## 1. Introduction

Oxygen consumption is one of the most important indexes of biological activity during cell culture and microbial development. Among the various tools to determine oxygen, the Clark-type oxygen sensor is the most widely used and has been applied in clinical analysis, fermentation monitoring, and biosensor development [1]. In the past two decades, owing to the progress in semiconductor and micromachining techniques, various types of miniature Clark-type oxygen sensors have been proposed [2–12]. It is necessary to consider the following aspects for fabricating a reliable sensor: (1) the fabrication and configuration of electrochemical electrodes in order to reduce the electrochemical crosstalk between different electrodes, (2) miniaturization techniques of the reference electrode for a longer lifetime and a more stable potential, (3) fixation and characteristics of internal electrolyte using different hydrogels or various types of electrolytes, and (4) bonding strategies and durability of the oxygen-permeable membrane and the detector substrate. Suzuki and coworkers

have significantly improved the above aspects [3–11] and employed the sensors practically in biological measurements [12–14].

Immobilized organisms and enzymes placed on the Clark oxygen sensor have been used as various biosensors. Most of these sensors still require to be dipped in a sample solution in order to detect the oxygen consumption of the immobilized biomaterials [14]. This dipping measurement requires a certain amount of sample solution (several milliliters) and expensive biochemical reagents. Recently, the micro total analysis system ( $\mu$ -TAS) has attracted widespread attention due to its excellent potential for offering highly efficient and simultaneous analysis of biological molecules or metabolisms by integrating the sensing system with the microfluidic system [15]. However, to date, the miniaturized Clark oxygen sensor has not been integrated with microfluidic systems or other microstructures.

In this study, we propose a novel micromachining technique to integrate the miniature Clark oxygen sensor with a microliter container and evaluate the characteristics of this innovative Clark oxygen sensor. Moreover, the oxygen consumption of bacterial suspension samples is practically evaluated by using the miniature Clark oxygen sensor.

\* Corresponding author. Tel.: +81 22 217 7281; fax: +81 22 217 6167.  
E-mail address: matsue@bioinfo.che.tohoku.ac.jp (T. Matsue).

## 2. Experimental

### 2.1. Materials

Slide glasses with a thickness of 1.8 mm purchased from Matsunami were used as the electrode substrate. A negative photoresist, SU8-2025 MicroChem, was used for lead insulation and in the micromachining structure. Silpot 184W/C poly(dimethylsiloxane) (PDMS) purchased from Dow Corning was used for the oxygen-permeable membrane. Sulfuric acid ( $\text{H}_2\text{SO}_4$ , Wako) and hydrogen peroxide ( $\text{H}_2\text{O}_2$ , Wako) were used for cleaning the slide glasses, and 2-propanol (Kanto Chemical) was used for cleaning the polyacrylate materials. All chemicals were of reagent grade and were used without further purification.

### 2.2. Fabrication and configuration of the electrodes

The structure of the oxygen sensor, consisting of a glass substrate and a PDMS container, was  $18\text{ mm} \times 26\text{ mm}$  as shown in Fig. 1. The glasses were first cleaned by immersing them in Piranha solution (3:7 of 96%  $\text{H}_2\text{SO}_4$  and 30%  $\text{H}_2\text{O}_2$ ) for 30 min. The lift-off technique was used to pattern the electrode geometry on the glass substrate, and 60 nm Ti and 260 nm Pt were sequentially sputter-deposited to be the working, reference, and counter electrodes. Subsequently, a 35  $\mu\text{m}$  thick insulator layer, fabricated using a SU8-2025 negative photoresist with 2000 rpm for 30 s, was used to define the sensitive area of the electrodes and simultaneously form a groove for the electrolyte solution (Fig. 1(a)). The area of the working electrode was  $20\text{ }\mu\text{m} \times 20\text{ }\mu\text{m}$  and that of the counter and reference electrodes was  $200\text{ }\mu\text{m} \times 2\text{ mm}$ . The application of a groove with a minimum width of 100  $\mu\text{m}$  reduced the crosstalk effect between the three electrodes during electrochemical detection by separating and connecting the different electrodes [7]. The peripheral region of the glass substrate outside the insulator was 2.5 mm in width; it

could be readily bonded with the PDMS container by an  $\text{O}_2$  plasma treatment.

### 2.3. Fabrication of oxygen-permeable membrane and PDMS container and its bonding to glass substrate

The oxygen-permeable membrane was prepared from a PDMS-curing agent mixture (10:1 w/w) due to its good oxygen permeability [16]. Furthermore, toluene was added at various concentrations to the PDMS mixture for adjusting the mixture viscosity in order to obtain PDMS membranes of varying thicknesses. A flat polyacrylate plate ( $38\text{ mm} \times 26\text{ mm}$ , Mitsubishi Rayon) was cleaned using 2-propanol with sonication for 3 min. The PDMS–toluene mixture was spread on the clean polyacrylate plate, spun at 5000 rpm for 60 s, and then cured on a hot plate at  $70\text{ }^\circ\text{C}$  for 10 min to form a membrane. The PDMS container was replicated from a home-made cone-type mold made from a polyacrylate material. The top-side diameter of the cone-type mold was 1.5 mm; it regulated the sensitive area of the oxygen sensor. The cone-type mold was removed to form a container after the curing process at  $70\text{ }^\circ\text{C}$  for 2 h. The PDMS container substrate was cut in suitable dimensions to fit the size of the glass substrate as shown in Fig. 1(b). Subsequently, both the PDMS membrane and the PDMS container were simultaneously treated with  $\text{O}_2$  plasma (100 W, 15 s). The PDMS container was then placed on the  $\text{O}_2$  plasma-treated membrane formed on the polyacrylate plate. The irreversible cross-linking between the  $\text{O}_2$  plasma treated surfaces resulted in the strong adhesion of the two materials [17]. Finally, the PDMS–container substrate was peeled off from the PDMS-coated plate. The irreversible adhesion between the PDMS materials formed the container with a thin PDMS membrane at the bottom for an oxygen-permeable membrane.

After drilling the inlets of the internal electrolyte, the PDMS substrate (Fig. 1(b)) was aligned and bonded with the glass substrate again by the  $\text{O}_2$  plasma treatment (100 W, 20 s). While the SU8 insulator area of the glass substrate exhibited a hydrophobic adhesion force with the PDMS substrate, the peripheral region of the glass substrate exhibited an irreversible bonding with the PDMS substrate to form a tough sealing.

### 2.4. Evaluation of sensor characteristics

We used a 0.1 M KCl/25 mM bicarbonate buffer solution (pH 9.5) as the internal electrolyte. Before bonding the glass substrate, the Pt quasi-electrode was electrochemically cleaned by alternatively applying a potential of +1.0 and  $-1.0\text{ V}$  versus Ag/AgCl (saturated KCl) for 30 s. It was not difficult to introduce the electrolyte solution into the long narrow groove. First, a layer of water covered the surface of the container. The water layer could prevent masses of gas from penetrating into the electrolyte groove during the application of suction. Subsequently, one of inlets was filled with the electrolyte, and the other inlet was subjected to

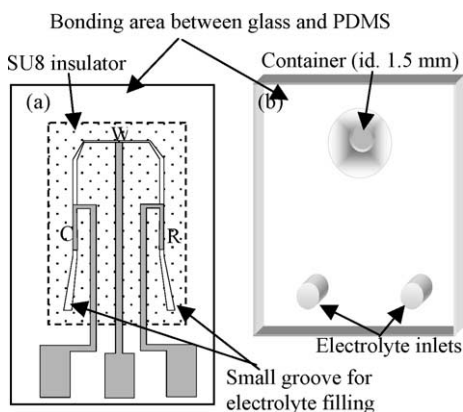


Fig. 1. The structure of a miniature Clark oxygen sensor. It consists of (a) a glass substrate with a groove made by SU8 photoresist and (b) a container substrate with an oxygen-permeable membrane. W, C and R are working, counter and reference electrode, respectively.

suction with a hand-held syringe. Since the groove surface had been treated with O<sub>2</sub> plasma during bonding, it became slightly hydrophilic to facilitate the electrolyte introduction. A three-electrode system connected with a potentiostat (HA-1010mM8, Hokuto-Denko) was used to evaluate the characteristics of the oxygen sensor. In order to test the linearity and durability, the sensitive area of the oxygen sensor was immersed in a 40 ml of 10 mM phosphate buffer solution (PBS) (pH 7.0) at room temperature. The dissolved oxygen concentration was varied by adding Na<sub>2</sub>SO<sub>3</sub>, and the concentration was simultaneously measured with an oxygen meter (Do-5509, Fuso-Rikaseihin). Additionally, a 100 mM Na<sub>2</sub>SO<sub>3</sub> solution at the zero-oxygen state was repetitively added to the container to test the reproducibility in air.

### 2.5. Preparation of bacterial suspension

The strain of *Escherichia coli* IFO3301 were purchased from the National Collection of Industrial and Marine Bacteria, Ltd. (NCIMB), Japan. Firstly, bacterial cells was cultured on the nutrient medium (pH 7.0) for 12 h at 36 °C. Colonies from this agar plate were transferred to a new agar plate with the sample components, and then cultured for 12 h at 36 °C. The nutrient agar medium comprises 5.0 g/l of beef extract, 10.0 g/l of peptone, 5.0 g/l of NaCl, and 15.0 g/l of agar in distilled water. After bacterial cells cultured for 12 h at 36 °C on the nutrient agar medium, the resulting colonies were suspended and diluted with different concentration in the PBS(–) buffer solution (7.2 mM Na<sub>2</sub>HPO<sub>4</sub>·12H<sub>2</sub>O, 2.8 mM KH<sub>2</sub>PO<sub>4</sub>, 150 mM NaCl, pH 7.0) with 100 mM D-(+)-glucose for the estimation of oxygen consumption.

## 3. Results and discussion

### 3.1. Fabrication of miniature Clark oxygen sensor

A micromachining technique was used to fabricate a stereo structure with deposited electrodes on a flat plane. It is advantageous to arrange the electrodes in a specific configuration and use channels to separate and connect different electrochemical electrodes in order to reduce the crosstalk between the electrodes in a low-volume electrolyte. The bonding strategies in the micromachining processes affect the packing or strength and the ability to integrate with different elements. Field-assisted bonding technique has been used to combine the glass and silicon substrates in the fabrication of micromachined Clark oxygen sensor [7]. However, field-assisted bonding requires a high electric voltage (kV) and high temperature (250 °C). It is detrimental to apply this technique to other semiconductor elements and polymer-material structures. Therefore, O<sub>2</sub>-plasma bonding was adopted to bond the oxygen-permeable membrane, the PDMS–container structure, and the glass substrate in this study. Moreover, the fabrication processes were conducted at relatively lower temperature conditions (<95 °C) compared with those of other

studies [7–12]. For example, instead of polyimide with a 300 °C curing temperature [8–12], SU8 photoresist was used as an insulator to form a groove. Additionally, the adhesion force of the oxygen-permeable membrane to the electrode surface also affects the durability of miniature Clark sensors. Generally, the membrane is immobilized with a physical adhesion force using dipping [4–6,8], spinning [3,9], casting [10], or glue-assisted techniques [2]. In the present fabrication, the oxygen-permeable membrane below the PDMS container readily and strongly adhered to the glass substrate due to the PDMS container-glass bonding. This greatly reduced the failure ratio which is usually high in dip- or spin-coating fabrication [3–6,8,9]. Fig. 2 shows the miniature Clark oxygen sensor with a container structure fabricated in this manner. Since the oxygen-permeable membrane resulted in complete separation of the internal solution in the groove from the outer solution in the container, the two different colored stains were not mixed. Further, due to sufficient adhesion force between the PDMS membrane and the SU-8 surface, there was no leakage of the internal solution from the groove edge. This method is feasible for directly integrating a microstructure with a miniaturized Clark oxygen sensor. It implies that the miniature Clark electrode can also be integrated with a microfluidic system to form a  $\mu$ -TAS chip. The distance between the oxygen-permeable membrane and the working electrode can be reduced using a thin insulator (SU-8). In the present chip, the membrane–electrode distance (approximately 35  $\mu$ m) is much smaller than that (200  $\mu$ m) of the other micromachining Clark sensors [7,9–12]. This configuration is highly important for the measurement of oxygen consumption of biological samples since the electrochemical response for oxygen increases when the electrode is located close to the oxygen-consuming biological samples.

Table 1 lists the characteristics of oxygen-permeable membranes fabricated under different conditions. The relation between the thickness of the oxygen-permeable membrane and the response time has been discussed in next section. Due to the high viscosity of the original PDMS mixture, the thickness could only be reduced to 15  $\mu$ m even at a spinning rate of 5000 rpm for 60 s. Therefore, toluene was used as

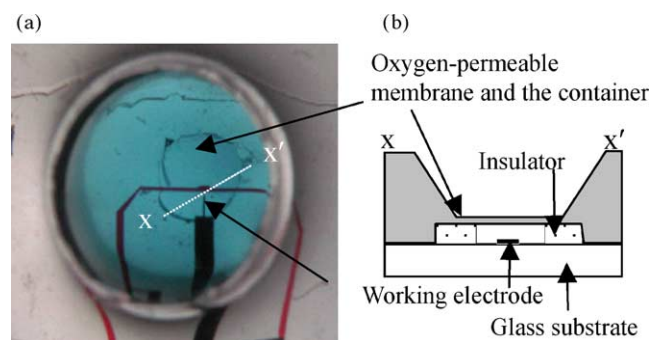


Fig. 2. (a) The top view of a miniature Clark oxygen sensor integrated with a container. (b) The cross-section along the line  $x-x'$  in (a). The container and the groove were filled with solutions containing blue and red stains, respectively.

Table 1  
Processing conditions of PDMS oxygen-permeable membranes

PDMS:toluene (w/w)	Spinning parameters		Thickness ( $\mu\text{m}$ )	90% response time (s)	
	rpm <sup>a</sup>	Time (s)		Range	Mean $\pm$ S.D. <sup>b</sup>
1:0	2000	60	31	25–30	27.3 $\pm$ 2.6
1:0	5000	60	15	6–14	8.7 $\pm$ 2.5
2:1	5000	60	7	3–10	6.8 $\pm$ 2.8

<sup>a</sup> rpm: revolutions per minute.

<sup>b</sup> S.D.: standard deviation ( $n = 15$ ).

a diluting solvent for PDMS in order to adjust the viscosity of the mixed solution. Toluene could be easily evaporated in the thermal curing step of the PDMS membrane, and the surface of the resultant membrane was smooth without obvious fractures or holes. In this study, a thin membrane with a thickness of only 3  $\mu\text{m}$  was fabricated using a PDMS–toluene solution in the ratio of 1:1 (w/w). Although we could successfully peel off the membrane from the polyacrylate plate by the  $\text{O}_2$  plasma bonding method, a thinner membrane would have been easily deformed due to the lack of mechanical strength against the adhesion force between the membrane and the supporting substrate. Therefore, the 3  $\mu\text{m}$  membrane was not used as the oxygen-permeable membrane. Additionally, it was worthwhile to note that the material of the substrates, on which the oxygen-permeable membrane was coated, ensures that the membrane remains intact when it is peeled off. In the case of a glass or silicon substrate, the strong adhesion force between the silicon substrate and the PDMS membrane causes the membrane to tear even if it has a thickness of 30  $\mu\text{m}$ . In contrast, the polyacrylate substrate greatly reduces the adhesion force of the PDMS membrane. Therefore, the mechanical strength of the membrane resists the adhesion force and maintains its appearance after it is peeled.

### 3.2. Characteristics of miniature oxygen sensor

#### 3.2.1. Cyclic voltammogram

Firstly, the electrochemical behavior of oxygen reduction in the miniature Clark oxygen sensor was investigated. Fig. 3(a) shows a typical cyclic voltammogram of oxygen reduction occurring in a miniature Clark oxygen sensor with an electrolyte solution of bicarbonate buffer (pH 9.5). The limiting current for oxygen reduction is observed to lie in the potential region of  $-0.5$  to  $-0.7$  V, indicating that the reduction current measured in the region can be used to estimate the oxygen concentration. As the potential becomes increasingly negative, hydrogen adsorption takes place at  $-0.78$  V. Hydrogen evolution occurs at higher negative potentials. Therefore, we employed  $-0.6$  or  $-0.7$  V potential to evaluate the electrochemical characteristics of the miniature Clark oxygen sensor. Fig. 3(b) shows the cyclic voltammograms for oxygen in the sensor with or without the 100 mM  $\text{Na}_2\text{SO}_3$  solution in the membrane-separated container. Since the  $\text{Na}_2\text{SO}_3$  solution filled in the container effectively removed oxygen in the measurement space, no reduction current for oxygen was observed. On the other hand, a well-defined current for oxy-

gen was seen in the air-filled container. The slight increase in reduction current at around  $-0.7$  V could be attributed to the  $\text{H}^+$  absorption on the Pt surface.

The Pt quasi-reference electrode functions as an anode during oxygen reduction at the cathode. Although the actual mechanism on the Pt reference electrode is not clear, we assume that it is related to the adsorption and oxidation reaction of  $\text{OH}^-$  on the Pt surface. Several studies have demonstrated

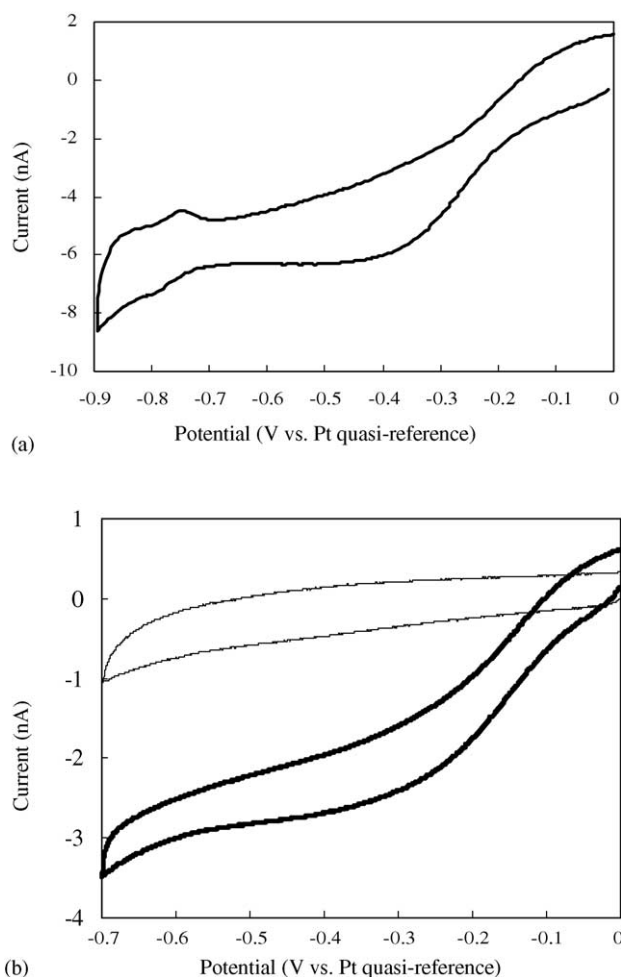


Fig. 3. Cyclic voltammogram of the miniature Clark oxygen sensor with a 15  $\mu\text{m}$  thick oxygen-permeable membrane. (a) Oxygen reduction current was measured in an air-filled container from 0 to  $-0.9$  V with a scanning rate of 50 mV/s. (b) The bold line shows the measurement in an air-filled container; while the thin line indicates the zero-oxygen state in a  $\text{Na}_2\text{SO}_3$ -filled container from 0 to  $-0.7$  V with a scanning rate of 10 mV/s.



that the  $\text{OH}^-$  is especially adsorbed and oxidized on a clean Pt surface in an alkaline solution [18–21]. The chemisorption ability of  $\text{OH}^-$  depends on the surface activity and pH value of the electrolyte [19–21]. This implies that the potential of the Pt quasi-reference electrode can be maintained within a stable range if the pH value of electrolyte is not altered or the Pt surface is not completely occupied with adsorbed  $\text{OH}^-$ . Unlike potentiometric electrodes, potential stability of the reference electrode might not be strictly required as long as the oxygen electrode is operated at the diffusion-controlled limiting current.

### 3.2.2. Stability and reproducibility

A  $\text{Na}_2\text{SO}_3$  solution with zero-oxygen concentration was employed to repetitively test the stability and reproducibility. These two characteristics of the sensor are closely related to the potential stability of the reference electrode and the crosstalk effect between the three electrodes of the electrochemical detector. Fig. 4(a) shows the response with peri-

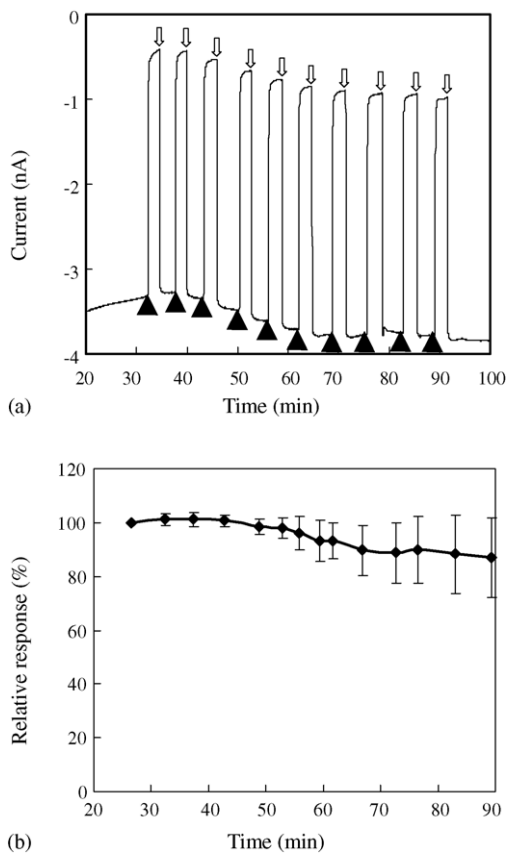


Fig. 4. Reproducibility and stability of the miniature oxygen sensor. The response was consecutively measured with periodic injection and suction of the  $\text{Na}_2\text{SO}_3$  solution from the membrane-separated container and suction of a Pt quasi-reference electrode with a  $15\ \mu\text{m}$  oxygen-permeable membrane. Solid and blank arrows show the container with and without the addition of  $\text{Na}_2\text{SO}_3$  solution, respectively. (a) The actual current response of a repetitive test and (b) mean  $\pm$  standard deviation of the relative responses to the first response with increasing time in five sensors. The first 20 min after the potential application are omitted.

odic injection and suction of the  $\text{Na}_2\text{SO}_3$  solution from the membrane-separated container of the miniature Clark oxygen sensor. Although the current baseline shifted slightly, the current response showed excellent reproducibility and it was maintained at the same level for 1.5 h. The baseline fluctuation within the first 60 min of potential application might be attributed to the change in surface status of the working electrode, such as hydrogen adsorption, and the change in potential shift of the reference electrode. If a gold working electrode and a micromachined Ag/AgCl reference electrode are used in this sensor, the stability will improve [9–12]. Fig. 4(b) shows the change in the relative current response to the first response in five miniature Clark oxygen sensors. Most of the sensors possessed an excellent reproducibility with only a 1% difference between the relative responses within the first 50 min of applying the potential. This phenomenon suggests that the electrode configuration by separating and connecting with a groove can effectively suppress the crosstalks between the working electrode and the counter electrode [7]. After 50 min, the difference of the relative responses from the first response gradually increased and reached 10%. This result might be caused by the overaccumulation of hydrogen peroxide on the working electrode as well as by the crosstalk between the byproducts from the counter electrode during continuous operation [4–7]. The fluctuation of the response can be retarded using a gel electrolyte [7]. Despite the fluctuation, a multi-comparative experiment can be conducted using this design with multi-working electrodes and containers on a chip within a stable period.

The 90% response time of the miniature Clark-type sensor with a  $15\ \mu\text{m}$  thick membrane was 8.7 s. The 90% response time increases with the thickness of the oxygen-permeable membranes in the sensor (Table 1). The response of the sensor with a  $7\ \mu\text{m}$  thick membrane was rapid (about 6.8 s). The rapid response is useful to monitor the kinetics of oxygen consumption of biological samples. It should be noted that the response time ( $<10\ \text{s}$ ) in this study was faster than that (about 1 min) of the other studies [5–12]. This fast response can be attributed to the reduced thickness, the membrane material, and a narrow gap between the oxygen-permeable membrane and the electrode surface.

### 3.2.3. Linearity

The sensitive area of the miniature oxygen sensor was immersed in 10 mM PBS (pH 7.0) for measuring the linearity. Fig. 5 shows the calibration curve for an oxygen sensor. Good linearity, with a correlation coefficient of 0.995, was observed due to the low electrochemical crosstalk between the three electrodes. The average residual current for zero oxygen concentration was 18% of the current measured in the solution with 7.9 ppm oxygen concentration. This value is larger than that measured in the three-electrode type micromachined Clark oxygen sensor [7]. The large residual current is possibly caused by the partial oxygen influx from the groove cavity, the influx of byproducts from the counter electrode, oxygen permeation from the PDMS top wall of the groove,

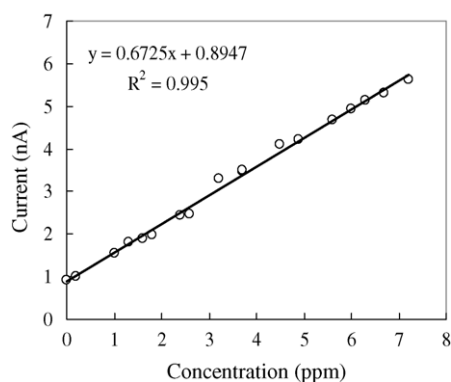


Fig. 5. Calibration curve for the miniature Clark oxygen sensor. The experiment was conducted in a 10 mM PBS solution (pH 7.0) by adding  $\text{Na}_2\text{SO}_3$ . Applied voltage:  $-0.7$  V.

and also by the specific adsorption of  $\text{H}^+$  on the Pt working surface. If the liquid electrolyte in this study is replaced by the solid-state proton conductive matrix [22] or the gel-like electrolyte [7,23], the residual current can be greatly decreased due to the low diffusion constant of oxygen in the solid-state electrolyte [22]. Another method to reduce the oxygen influx from the PDMS wall is to use a glass substrate instead of PDMS materials to form the microstructure layer.

### 3.2.4. Lifetime

The miniature Clark oxygen sensor was immersed in 10 mM PBS (pH 7.0) to investigate the sealing and lifetime. Fundamentally, if the bonding between the PDMS substrate and the glass substrate cannot produce a good sealing, the external PBS will flow into the groove and affect the pH value of the electrolyte. Since the pH value of internal electrolyte can stabilize the potential of the Pt quasi-reference electrode, the oxygen reduction current does not show a larger change. Fig. 6 shows the results of the lifetime tests at different potentials. The sensor was continuously operated for at least 60 h at  $-0.7$  V. The current obtained at  $-0.7$  V showed a better stability and a longer lifetime than that obtained at  $-0.4$  V.

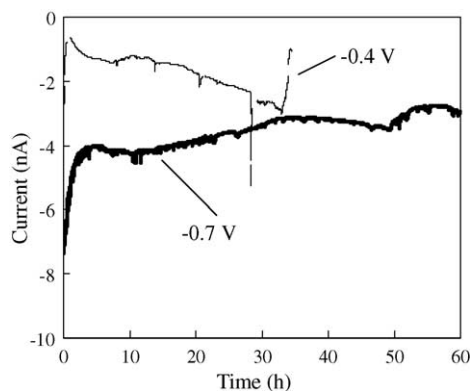


Fig. 6. Lifetime of the miniature oxygen sensor. The sensitive area of the sensor was immersed in 10 mM PBS (pH 7.0) to continuously monitor the output current. Bold and thin lines indicate an applied potential of  $-0.7$  and  $-0.4$  V, respectively.

Since the potential of  $-0.7$  V is in the limiting-current region, the slight potential shift of the Pt quasi-reference electrode only has a small effect on the oxygen reduction current. Further, the adhesion layer, titanium, is stable at this potential. A microscopy observation revealed that prolonged operation of the working electrode at  $-0.4$  V caused it to become transparent. A sudden decrease in the output current at 33 h caused fatal damage to the working electrode operated at  $-0.4$  V.

### 3.3. Oxygen consumption of different concentration *E. coli*

$20 \mu\text{l}$  *E. coli* suspensions of different concentration ( $10^{11}$ – $10^5$  cells/ml) and PBS(–) were separately injected into the membrane-separated container to estimate the oxygen consumption. Fig. 7 shows the time-courses of the normalized oxygen-reduction current before and after adding the tested solutions into the micro-container. The results showed that the higher concentration *E. coli* consumed a greater deal of oxygen. Presently, the Clark sensor in this study can repeatedly distinguish the *E. coli* concentration as low as  $10^5$  cells/ml ( $\sim 2000$  cells). If the residual current problem can be effectively eliminated to possess a better sensitivity, a lower concentration than  $10^5$  cells/ml is possibly detected. Moreover, the miniature Clark sensor directly integrated with micro-container is easier to manipulate the microliter-scale suspensions than those without the microstructure [2–12,22,23]. If a microfluidic channel is integrated with the Clark sensor by using the same fabrication processes, it has potential to develop a miniature flow-

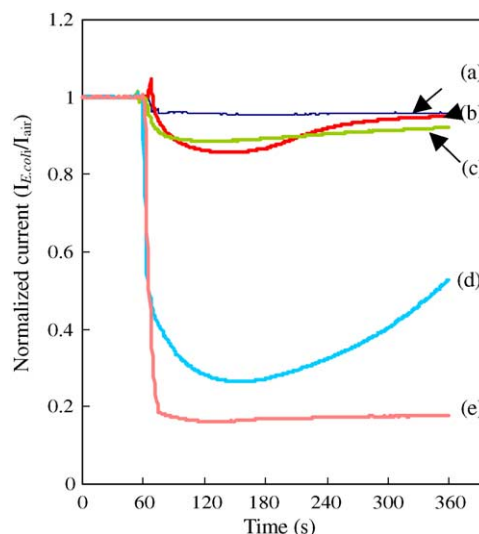


Fig. 7. The time-courses of the normalized oxygen-reduction current were monitored before and after adding (a) PBS(–), (b) *E. coli* suspension of  $2.3 \times 10^5$  cells/ml, (c)  $2.3 \times 10^7$  cells/ml *E. coli*, (d)  $2.3 \times 10^9$  cells/ml *E. coli*, (e)  $2.3 \times 10^{11}$  cells/ml *E. coli* into the membrane-separated container.  $I_{E. coli}$  and  $I_{\text{air}}$  are the oxygen-reduction currents measured with and without different concentration *E. coli* suspensions in the container, respectively. The volume of all tested suspensions is  $20 \mu\text{l}$  and is injected at around 60 s after beginning the record.

injection-analysis system to quickly detect the biological oxygen concentration.

#### 4. Conclusions

In this study, we presented a novel fabrication technique to combine the miniature Clark oxygen sensor with a membrane-separated container. The simple and low-temperature fabrication processes can be easily reproduced and integrated with other semiconductor elements and polymer structures in an ordinary laboratory. Using the thick-film technique with the SU8 photoresist, the detection electrode in the sensor is located close (35  $\mu\text{m}$ ) to the measurement container. In addition, the separation membrane for oxygen permeation is extremely thin (7  $\mu\text{m}$ ). Due to the thin membrane and the proximity of the measuring container to the detection electrode, the response of the sensor to a change in oxygen concentration is rapid (90% response time, 6.8 s). The faster response of the sensor is useful to monitor the kinetics of oxygen variation in biological samples. Although the present Clark oxygen sensor faces limitations in long-term measurement, it can be improved using a gel electrolyte and a more stable reference electrode. As previously mentioned, the most important potential application of the miniature Clark oxygen sensor is the integration of its functions with a microfluidic system to form a  $\mu$ -TAS for measuring single cells such as an embryo or a low-volume biological sample.

#### Acknowledgment

This work was partly supported by Grants-in-Aid for Scientific Research (15201030, 15033204) from the Ministry of Education, Science and Culture, Japan. We also gratefully acknowledge the partial financial support received from Yen Tjing Ling Foundation, Taiwan.

#### References

- [1] G.S. Wilson, *Bioelectrochemistry*, Wiley, New York, 2002, pp. 40–46.
- [2] M. Koudelka, Performance characteristics of a planar Clark-type oxygen electrode, *Sens. Actuators* 9 (1986) 249–259.
- [3] H. Suzuki, E. Tamiya, I. Karube, Fabrication of an oxygen electrode using semiconductor technology, *Anal. Chem.* 60 (1988) 1078–1080.
- [4] H. Suzuki, A. Sugama, N. Kojima, Miniature Clark-type oxygen electrode with a three-electrode configuration, *Sens. Actuators B* 2 (1990) 297–303.
- [5] H. Suzuki, N. Kojima, A. Sugama, F. Takei, K. Ikegami, Disposable oxygen electrodes fabricated by semiconductor techniques and their application to bioelectrodes, *Sens. Actuators B* 1 (1990) 528–532.
- [6] H. Suzuki, N. Kojima, A. Sugama, F. Takei, Development of a miniature Clark-type oxygen electrode using semiconductor techniques and its improvement for practical applications, *Sens. Actuators B* 2 (1990) 185–191.

- [7] H. Suzuki, A. Sugama, N. Kojima, Micromachined Clark oxygen electrode, *Sens. Actuators B* 10 (1993) 91–98.
- [8] Z. Yang, S. Sasaki, I. Karube, H. Suzuki, Fabrication of oxygen electrode arrays and their incorporation into electrodes for measuring biochemical oxygen demand, *Anal. Chim. Acta* 357 (1997) 41–49.
- [9] H. Suzuki, H. Ozawa, S. Sasaki, I. Karube, A novel thin-film Ag/AgCl anode structure for microfabricated Clark-type oxygen electrodes, *Sens. Actuators B* 54 (1998) 140–146.
- [10] H. Suzuki, T. Hirakawa, S. Sasaki, I. Karube, An integrated module for sensing pO<sub>2</sub>, PCO<sub>2</sub>, and pH, *Anal. Chim. Acta* 405 (2000) 57–65.
- [11] H. Suzuki, H. Arakawa, I. Karube, Fabrication of a sensing module using micromachined bioelectrodes, *Biosens. Bioelectron.* 16 (2001) 725–733.
- [12] H. Suzuki, T. Hirakawa, I. Watanabe, Y. Kikuchi, Determination of blood pO<sub>2</sub> using a micromachined Clark-type oxygen electrode, *Anal. Chim. Acta* 431 (2001) 249–259.
- [13] H. Suzuki, Microfabrication of chemical electrodes and bioelectrodes for environmental monitoring, *Mater. Sci. Eng. C: Biomimetic Supramol. Syst.* 12 (2000) 55–61.
- [14] Z. Yang, H. Suzuki, S. Sasaki, I. Karube, Disposable electrode for biochemical oxygen demand, *Appl. Microbiol. Biotechnol.* 46 (1996) 10–14.
- [15] S.J. Lee, S.Y. Lee, Micro total analysis system ( $\mu$ -TAS) in biotechnology, *Appl. Microbiol. Biotechnol.* 64 (2004) 289–299.
- [16] F. Mizutani, S. Yabuki, T. Sawaguchi, Y. Hirata, Y. Sato, S. Iijima, Use of a siloxane polymer for the preparation of amperometric electrodes: O<sub>2</sub> and NO electrodes and enzyme electrodes, *Sens. Actuators B* 76 (2001) 489–493.
- [17] J.C. McDonald, D.C. Duffy, J.R. Anderson, D.T. Chiu, H.K. Wu, O.J.A. Schueller, G.M. Whitesides, Fabrication of microfluidic systems in poly(dimethylsiloxane), *Electrophoresis* 21 (2000) 27–40.
- [18] A.V. Tripković, K.D. Popović, J.D. Lović, The influence of the oxygen-containing species on the electrooxidation of the C<sub>1</sub>–C<sub>4</sub> alcohols at some platinum single crystal surfaces in alkaline solution, *Electrochim. Acta* 46 (2001) 3163–3173.
- [19] E. Gasana, P. Westbroek, E. Temmerman, H.P. Thun, F. Twagiramungu, Influence of changes of platinum electrode surface condition on the kinetics of the oxidation of sodium dithionite and sulfite in alkaline solution, *Electrochem. Commun.* 2 (2000) 727–732.
- [20] D.M. Dražić, A.V. Tripković, K.D. Popović, J.D. Lović, Kinetic and mechanistic study of hydroxyl ion electrosorption at the Pt(111) surface in alkaline media, *J. Electroanal. Chem.* 466 (1999) 155–164.
- [21] A.V. Tripković, K.D. Popović, J.D. Lović, D.M. Dražić, Kinetic and mechanistic study of methanol oxidation on a Pt(111) surface in alkaline media, *J. Electroanal. Chem.* 418 (1996) 9–20.
- [22] G.W. McLaughlin, K. Braden, B. Franc, G.T.A. Kovacs, Microfabricated solid-state dissolved oxygen sensor, *Sens. Actuators B* 83 (2002) 138–148.
- [23] M. Wittkamp, G.C. Chemnitz, K. Cammann, M. Rospert, W. Mokwa, Silicon thin film sensor for measurement of dissolved oxygen, *Sens. Actuators B* 43 (1997) 40–44.

#### Biographies

**Ching-Chou Wu** received a PhD degree in Institute of Biomedical Engineering, Cheng-Kung University, Taiwan. In 2003, he joined Matsue's laboratory in the graduate School of Environmental Studies, Tohoku University as a post doctor fellow. His current interest is the fabrication and integration of microsensors with microfluidic systems.

**Tomoyuki Yasukawa** received his PhD degree in engineering from the Tohoku University, Japan, in 2000. He is working as a research assistant, in the Graduate School of Environmental Studies, Tohoku University, Japan.

**Hitoshi Shiku** did his PhD in engineering from the Tohoku University, Japan, in 1997. He is working as an assistant professor, in

the Graduate School of Environmental Studies, Tohoku University, Japan.

**Tomokazu Matsue** earned his PhD in pharmacy in 1981, and he is currently working as a professor in Graduate School of Environmental Studies, Tohoku University, Japan.